NC STATE UNIVERSITY

College of Engineering
Department or Nuclear Engineering
Nuclear Reactor Program
www.ne.ncsu.edu/nrp

Campus Box 7909
2500 Stinson Drive
Raleigh, NC 27695-7909
P: 919.515.7294

December 31, 2015

U.S. Nuclear Regulatory Commission
Document Control Desk
Washington, DC

SUBJECT **RESPONSE SUBMITTAL 2 TO THE REQUEST FOR ADDITIONAL INFORMATION FOR TECHINCAL SPECIFICATION AMENDMENT 19 – USE OF 6% ENRICHED FUEL**
License No. R-120
Docket No. 50-297

Please find enclosed submittal 2 of the response to the Request for Additional Information (RAI) for the License Amendment Request (LAR) related to the use of six percent enriched fuel (TAC NO. MF6088). This submittal supplies the response to RAI question 4.

If you have any questions regarding this amendment or require additional information, please contact Andrew Cook at (919) 515-4602 or atcook@ncsu.edu.

I declare under penalty of perjury that the forgoing is true and correct. Executed on 31 December 2015.

Sincerely,

Ayman I. Hawari, Ph.D.
Director, Nuclear Reactor Program
North Carolina State University

Enclosures: Submittal 2 – Response to Request for Additional Information

RESPONSE TO REQUEST FOR ADDITIONAL INFORMATION
FOR LICENSE AMENDMENT REQUEST FOR
THE USE OF SIX PERCENT ENRICHED FUEL (TAC NO. MF6088)

SUBMITTAL 2

NORTH CAROLINA STATE UNIVERSITY
LICENSE NO. R-120; DOCKET NO. 50-297
DECEMBER 31, 2015

Question 4: Appendix A, Section 3.1, of the NCSU LAR describes the general purpose Monte Carlo N-Particle code (MCNP6) model used to evaluate the steady-state neutronic characteristics of the PULSTAR reactor. The guidance in NUREG-1537, Part 2, Section 4.2, "Reactor Core," and Section 4.5, "Nuclear Design," states, in part, that the applicant should present all design information and analyses necessary to demonstrate that the core can be safely operated. Please provide the following information:

Consistent with the guidance in NUREG-1537, Part 2 Sections 4.2 and 4.5, the objective of the MCNP6 analysis has been to demonstrate that PULSTAR reactor core configurations that are loaded with fuel enriched to both 4% and 6% (in uranium 235) continue to adhere to the limits set in the PULSTAR's Technical Specifications. Therefore, it is fully expected that the PULSTAR reactor will continue to operate safely and reliably while staying within the licensing basis of the current Safety Analysis Report

As discussed in the license amendment request (LAR), the fuel loading approach for new mixed enrichment (4% and 6%) core configurations will be:

1) Use the established MCNP6 model to predict a core loading pattern that meets the licensed technical specifications limits.
2) Configure the core according to the predicted loading pattern.
3) During startup testing, use existing procedures to confirm the MCNP6 predictions of maximum worth of a single fuel assembly, total nuclear peaking factor, shutdown margin, excess reactivity, and rate of reactivity insertion of the control rods.
4) If any of the quantities in step 3 do not meet the licensed technical specifications limits, the reactor will be shut down.

The above approach will be implemented using established PULSTAR reactor procedures. Step 3 implements these procedures to verify (by measurement) the predicted key parameters for new mixed enrichment (4% and 6%) core configurations prior to operating at full power.

The specific issues that are raised in relation to this question are discussed below.

a) Discuss the details/assumptions made on how the fuel assembly was modeled. Explain how the fuel assembly cells (material/geometry) were treated and tracked during the depletion calculations.

The MCNP6 model geometry of the PULSTAR was constructed explicitly from original equipment manufacturer (OEM) specifications [1-4]. All the implemented dimensions of

fuel assembly components and the core loading were within the OEM tolerances. Fuel materials were also specified within the tolerances of OEM specifications. Tables 1-5, detail the OEM specifications and corresponding MCNP6 geometry and material properties. Generally, the variation of values within the OEM specified tolerances proved helpful in enhancing agreement between MCNP6 predictions and measurements. MCNP6 uses combinatorial geometry to model reactor systems, whereby basic geometric shapes are used to define material containing volumes which are the building blocks of the reactor. The general methodology for modeling of the PULSTAR is as follows:

1) Define a the basic cylindrical fuel volume, clad and coolant channel
2) Construct a fuel pin-channel unit by 'stacking' 10 fuel volumes within a clad inside the coolant channel. In this case each of the 10 fuel volumes was defined to be unique
3) Define an assembly box and fill it with a lattice of 25 fuel pin-channel units. Each of the 10 fuel volume units in each pin-channel unit is uniquely redefined from the basic pin-channel unit and given a new material, as it was filled into the assembly. The resulting combined geometry was defined as an assembly. A total of 25 unique assemblies were explicitly defined for each core.
4) Define the auxiliary core components (e.g. control rods, grid plate, etc.)
5) Define all reflectors which will occupy core positions (e.g. graphite, beryllium, or water-hole)
6) Fill the core lattice with the 25 assemblies and reflectors corresponding to the core configuration to construct the reactor core

Table 1. Fuel Pin Geometry.

Parameter	OEM Specifications	Value in MCNP6 Model
Pellet Diameter	0.423" (±0.002")	0.423"
Diametrical Gap	0.0085" (±0.001")	0.0085"
Outer Diameter	0.4725" (±0.002")	0.474"
Height of Pellet Stack	24" (±0.015")	24"
Rectangular Spacing	0.521" × 0.603" (±0.001")	0.522" × 0.604"
Clearance, Pin to Pin	0.051" × 0.133" (±0.003")	0.048" × 0.13"

Table 2. Fuel Pin Material Properties (4% in ^{235}U).

Parameter	OEM Specifications	Value in MCNP6 Model
Enrichment	4% ± 0.056%	4.026% (value given in PULSTAR reports)
Density	10.4-10.76 g/cm^3	10.407 g/cm^3
Weight of UO_2	572 g ± 11 g	575 g

Table 3. Fuel Pin Material Properties (6% in ^{235}U).

Parameter	OEM Specifications	Value in MCNP6 Model
Enrichment	6% ± 0.056%	6.000%
Density	10.2-10.7 g/cm^3	10.405 g/cm^3
Weight of UO_2 per pin	582 g ± 12 g	575 g

Table 4. Fuel Assembly Geometry.

Parameter	OEM Specifications	Value in MCNP6 Model
Inside Dimensions	2.620" × 3.030" (±0.010")	2.610" × 3.020"
Wall Thickness	0.060" (±0.005")	0.065"
Clearance, Pin to Box	0.025" × 0.066" (±0.020")	0.024" × 0.065"
Clearance between Assemblies	0.040" (±0.007")	0.039"
Clearance between control Rod Guide and Assemblies	0.060" (±0.016")	0.0585"

Table 5. Control Rod Geometry.

	OEM Specifications	Value in MCNP6 Model
Guide Area	0.438" × 6.34" (±0.031")	0.44" × 6.34"
Absorber Area	0.180" × 4.85" (±0.015")	0.18" × 4.85"
Clearance, Absorber to Guide	0.025" × 0.066" (±0.017")	0.024" × 0.065"

The cell cards in the PULSTAR model were laid out in two sections. The first section defines all elementary core components, including fuel pellets and water channels. The second section defines the construction of each fuel assembly. These sections are separated by a lattice definition card which defines the core configuration, i.e. the assembly and reflector locations. Cell cards containing water or inside the core included a TMP card to define the temperature of the material within that cell. Additionally fuel cells included an explicit definition for the volume. The most important cell definitions for the analysis performed in this work are those for control rods, beam-tubes, nosepiece, and fuel.

Each control rod is defined independently and labeled according to their alpha-numeric position in the core, e.g. the shim rod is between D4 and D5. These controls rods may be moved by changing the cell cards defining the top and bottom. The beam-tubes are clearly labeled, and each beam-tube may be defined to be filled with water (default) or defined to be empty. The empty state of a beam-tube (or a coolant channel) was defined to be void. The modeling of beam-tubes as void may simulate the draining of the beam-tubes for the estimation of beam-tube worth. The definitions for nosepiece are labeled and defined with

a lattice definition complementary to that for the fuel assemblies, but located directly below the fuel lattice definition.

Each grid plate position (A1-F6) is replaced by the cell card corresponding to the component in that position in the core configuration considered, e.g. RC1 or RC8. These components may be reflectors, water column, or fuel assemblies. In this work each reflector type and water column had a unique cell number as to allow each component to be interchanged for any core. Graphite reflectors are designated by cell number 6, beryllium reflectors by 7, and water columns by 5. Fuel assemblies are designated by a cell number computed as (10 + 'Assembly Number')×1000, e.g. the cell number for assembly 1 is 11000.

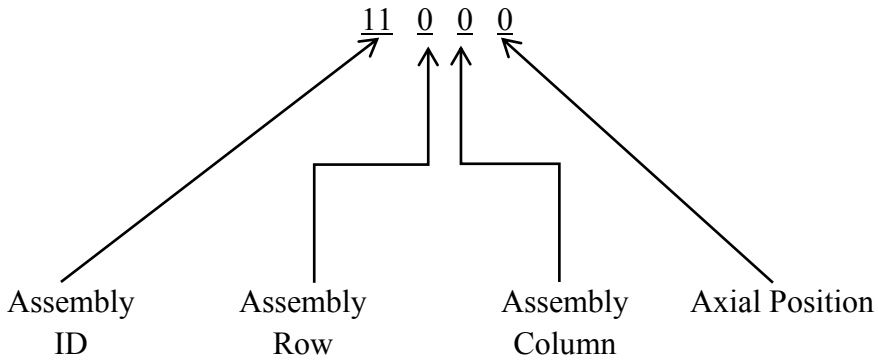

To accurately simulate the change in material composition as a function of position and core configuration over the operational history of the PULSTAR, each fuel pin was uniquely defined and subdivided into 10 unique axial cells. Each fuel cell was defined with a unique material, density, and given a unique ID number corresponding to its assembly, pin, and axial position.

The assembly ID for the fuel pin is the assembly designation number plus 30. The row number starts at 0 for fuel pins closest to the F-row side of the core and is indexed by 1 for each successive row. The column number starts at zero for the fuel pins closest to column 1 side of the core and is indexed by two for each successive column. The axial position starts from 0 at the bottom of the core and is indexed by 1 for each successive discrete axial position. The example shown below is for the fuel cell at the bottom of assembly 1 in the first row and first column (the pin position closest to the F1 corner of the core). Each fuel cell was defined with a unique material card to ensure that the corresponding material was moved correctly with the fuel cell during core shuffling. The material ID number corresponding to an assembly, pin and axial position was defined as shown below. The assembly ID for the fuel pin material is the assembly designation number, but all other components of the material ID is the same as the corresponding fuel pin ID.

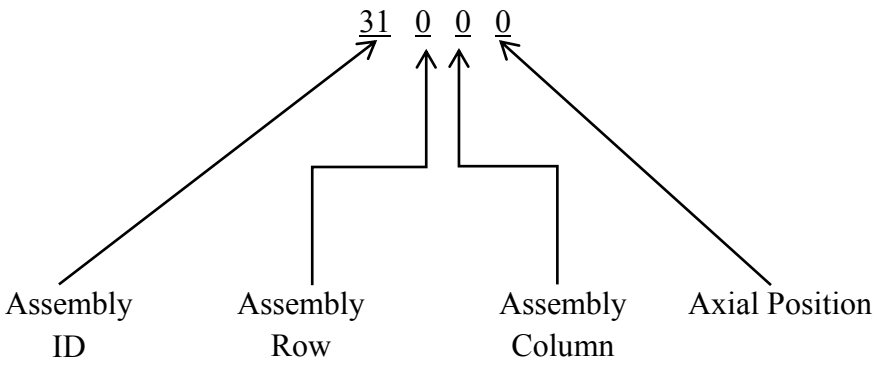

b) Discuss whether the effects of manufacturing tolerances for the fuel assembly were considered in the analysis.

The effects of manufacturing tolerances were considered in the modeling of the PULSTAR. The dimensions of the assembly and its components as well as reflectors and control rods were set according to OEM specs. When necessary the dimensions and material properties were adjusted within OEM tolerances to provide results most consistent with measurements. This includes both reactivity related measurements (e.g. excess reactivity) and physical measurements of the geometry of core components. This adjustment process was performed for the standard core for all basic components. Adjustments to reflectors were performed for the first core in which the reflector was used. The variations in core pin peaking factor (nearly 2%) and excess reactivity due to the variation in the pitch and diameter of the fuel pins for the standard core, RC8 and RC9-2 (see Appendix A for naming conventions) were well within the margins given in Appendix A. Similar results were also obtained for the variation in core pin peaking factor and excess reactivity due varying the fuel pin mass in the standard core and RC9-2 respectively. Tables 1 through 5 above show the data used in the MCNP 6 model in comparison to OEM specifications.

c) Address how the statistical variations were addressed in the calculations. (For example, was the average value of 10 runs with varying random number generator utilized?)

Statistical variations were reduced through the use of sufficiently large number of particles to reduce uncertainty in reactivity to less than 10 pcm and relative uncertainty in the F7 tally (fission energy deposition) to less than approximately 1%. A sufficient number of inactive kcode cycles were run to guarantee that the Shannon entropy (i.e. fission entropy) was well converged (e.g., sufficient to pass the entropy statistical check). In this case, the number of inactive kcode cycles is at least an order of magnitude greater than the minimum required; where the minimum number of cycles is the first cycle in which the Shannon entropy is within one standard deviation of the running average. The number of inactive cycles was set sufficiently high that the estimated final k_{eff} was predicted to vary by less than 1σ in k_{eff} with additional inactive cycles for criticality and burn-up calculations.

d) Discuss how the model statistics (e.g., minimizing the calculation uncertainty) were addressed and verification of fission occurring were checked for in each cell.

The kcode parameters were set to provide reasonable neutron generation statistics within each of the 6250 cells modeled for the PULSTAR fuel. For reactor safety related calculations the number of neutrons per kcode cycle was set to 100,000, which on average is expected to result in the generation of 16 source points in each of the 6250 cells modeled for the PULSTAR fuel for each cycle. In addition, the number of stored source points was set to 300,000, which on average is expected to result in 48 stored source points in each fuel cell. These parameters were selected to reduce the change in the neutron source distribution and k_{eff} from cycle to cycle. For both burn-up calculations and reactor safety related calculations, a script was written to verify that fission occurred during kcode analysis in each fuel volume cell of each core configuration.

For reactor safety related calculations the script, `tally_check.sh`, verified that every unique F7 and F4 tally for each unique fuel volume cell in the file `coreID_peakingfactors.mctal` was not equal to zero. This script generates the file, `tally_check.out`, which indicates whether the tallies pass or fail this test. The `coreID` refers to the prefix identifying the core configuration (e.g. `st`, `rc1`, `rc8`, etc.).

For burn-up calculations the fission rate of ^{235}U in each unique volume cell predicted for a burn-up step was extracted from `coreID_burn.out` using the command

```
grep “list_ID 92235” coreID_burn.out > coreID_fission_check.dat
```

The `list_ID` is unique to each core configuration and indicates the position of ^{235}U in a monotonically increasing list of isotopes tracked in the fuel by their atomic number, Z, and mass, A. The script, `burn_check.sh`, verified that the fission of ^{235}U was none zero for each occurrence in `coreID_fission_check.dat` (i.e. column 5 of every other row, corresponds to fission). This script generates a file, `burn_check.out`, which indicates whether the fission rates pass or fail this test.

e) Explain how the MCNP6 calculated statistical uncertainty was applied to the core reactivity parameter and power peaking results.

Statistical uncertainty was estimated for the core reactivity parameters and power peaking results through propagation of error analysis. The uncertainty in k_{eff} (as given by MCNP6) may be propagated into the predicted reactivity as

$$\sigma_\rho = \sqrt{\left(\frac{\sigma_{k_{eff}}}{{k_{eff}}^2}\right)^2} \qquad (1)$$

Table 6. Summary of statistical uncertainty for various reactor parameters. The uncertainty limit for each parameter is the maximum statistical uncertainty calculated for any core. The ratio between calculated and experimentally measured values (C/E) was chosen as the average for each parameter.

	Statistical Uncertainty Limit	C/E
α_T	± 0.026	0.91
α_F	± 0.014	1.03
α_V	± 0.020	0.73
α_P	± 0.013	1.04
k_{eff}	± 2E-5	1.001
ρ_{excess}	± 0.011	1.05
β_{eff}	± 0.017	1.02
S1	± 0.006	1.11
S2	± 0.006	1.13
Reg	± 0.006	1.10
Shim	± 0.006	1.02
Gang	± 0.003	1.11
SDM	± 0.0021	1.17
$\dot{\rho}$ (pcm/s)	± 0.011	0.86
F_Q	± 0.006	0.96
F_Q^A	± 0.002	0.96

Relative uncertainty in the F7 tallies was propagated into the pin power peaking factor, F_Q, as,

$$\frac{\sigma_{F_Q}}{F_Q} = \sqrt{\sum_{i \neq m} \left(\frac{D_i \tilde{\sigma}_i}{\sum D_i} \right)^2 + \left(\sigma_m - \frac{D_m \tilde{\sigma}_m}{\sum D_i} \right)^2} \qquad (2)$$

where D_i is the F7 tally in the ith unique fuel volume cell with a relative uncertainty $\tilde{\sigma}_i$. The index m identifies the fuel volume cell with the greatest F7 tally value, which is representative of the 'hottest' pellet in the core.

The uncertainty in reactivity was propagated into the uncertainty of reactivity feedback coefficients using the linear fit model (as seen in Appendix A, page 13, Equation 4-2),

$$\rho = \rho_{excess} + \alpha_G \Delta G \tag{3}$$

The resulting uncertainty in α_G, is

$$\sigma_{\alpha_G} = \sqrt{\sum \left(\frac{\sigma_{\rho_i} \left(NG_i - \sum G_i \right)}{N \sum G_i^2 - \left(\sum G_i \right)^2} \right)^2}, \tag{4}$$

where N is the number of data points, G_i is the variable defining the core state for the feedback coefficient, and $\sigma_{\rho i}$ is the uncertainty in the corresponding reactivity (see Eq. 3). The uncertainty limits for the core parameters are summarized in Table 6 above.

f) Provide justification for why the 15 percent margin added to the calculated peaking factor for mixed enrichment cores provides sufficient confidence that the observed peaking factor will not exceed the limit in TS 3.1.f., given that the experimental margin was determined from uniform enrichment experiments only.

The 15% margin was derived from the observed relative deviation between the calculated and experimentally measured peaking factors for the 8 benchmark cores of the PULSTAR reactor (i.e., the standard core through the currently operating reflected core 8). Table 3.2 in Appendix A of the submitted LAR gives the data used in this analysis. Based on this data the deviation was determined for each of the eight cores. Statistical analysis of the resulting relative deviation gives

Average relative deviation = 1.068 (i.e., 6.8%)
Standard deviation of the data (S) = ±0.042 (i.e., 4.3%)
Standard error of the average relative deviation (σ) = ±0.015 (i.e., 1.5%)

Based on the above, a 4σ limit (i.e., 4 times the standard error of the average) for the deviation can be set at 1.13, which based on the assumption of a Gaussian distribution of the data gives a 99.99% confidence level that a calculated value of the peaking factor will not deviate by more than 13% from an observed value. To be conservative the limiting deviation was set to 1.15, which represents the upper limit observed in the data. Assuming that the 2.92 limit set in the PULSTAR Technical Specifications represents an observed value, the limiting calculated peaking factor is found to be 2.54, which supports the conclusion that cores RC9-1 and RC9-2 are acceptable (see Table 4.2 and Figures 4.5 and 4.6 of Appendix A in the submitted LAR).

The above analysis derives the peaking factor limit directly from the data and without any assumptions about the statistical distribution of the data except for estimating the confidence level. For that purpose, using other distributions (such as the Student t distribution) results in setting similar confidence levels. Furthermore, this analysis inherently accounts for all the potential sources of uncertainty and bias in both calculation

and measurement as the "observed deviation" is a quantity that represents the convolution of all such contributors to data fluctuations and deviations.

Finally, it can be seen from Table 4.2 and Figures 4.5 and 4.6 in Appendix A of the LAR that reflected cores RC9-1 and RC9-2 have generally similar power distributions to the current reflected core RC8. Therefore, the power peaking behavior for RC9-1 and RC9-2 should be similar to RC8 as predicted by the MCNP6 simulations and given in Table 4.2.

g) The uncertainty margin is the difference between the experimental measured results and the MCNP6 calculated result.

1) Explain how the MCNP6 code utilizing the ENDF/B-VII cross-sections libraries was validated and the associated uncertainty margin was addressed.

The locally implemented MCNP6 code (and its default ENDF/B-VII based cross-section libraries) was validated by running the test suites available with the distributed MCNP6 code package. The outcome of running the test suites indicated that no differences were found between the implemented MCNP6 code and the results provided with the MCNP6 code package data for all cases relevant to kcode and particle tracking simulations. Any differences found in the tests suites were due to computational precision, and were found only for modules of MCNP6 related to physics models not utilized in this work.

Cross section libraries generated with NJOY99 for use in MCNP6 were validated through comparison to the default MCNP6 libraries, as well as careful verification of the NJOY inputs. The comparison between default MCNP6 libraries and those generated through NJOY99 may be exemplified graphically, in which the expected behavior of processed nuclear data libraries (e.g. due Doppler broadening) are observed.

Total cross-sections corresponding to H in H_2O S(α,β) library generated using NJOY are compared to the MCNP6 libraries at 68.8 ºF (lwtr.60t) and 260 ºF (lwtr.61t) in Figures 1 and 2 respectively. The temperature at which each library was processed is listed in Table 7. The default MCNP6 libraries are lwtr.60t and lwtr.61t, which were originally processed with NJOY99. Libraries for H in H_2O demonstrate an increasing total cross-section with increasing temperature, approaching a 1/v behavior at low energies. As expected all cross-sections are between the 68.8 ºF and 260 ºF MCNP6 libraries, with the 70 ºF (h0700f.00t) approximately equal to the lwtr.60t library.

Table 7. LWTR Thermal Cross-Section Libraries.

Library	Temperature (°F)
lwtr.60t	68.8
lwtr.61t	260
h0700f.00t (this work)	70
h1000f.00t (this work)	100
h1050f.00t (this work)	105

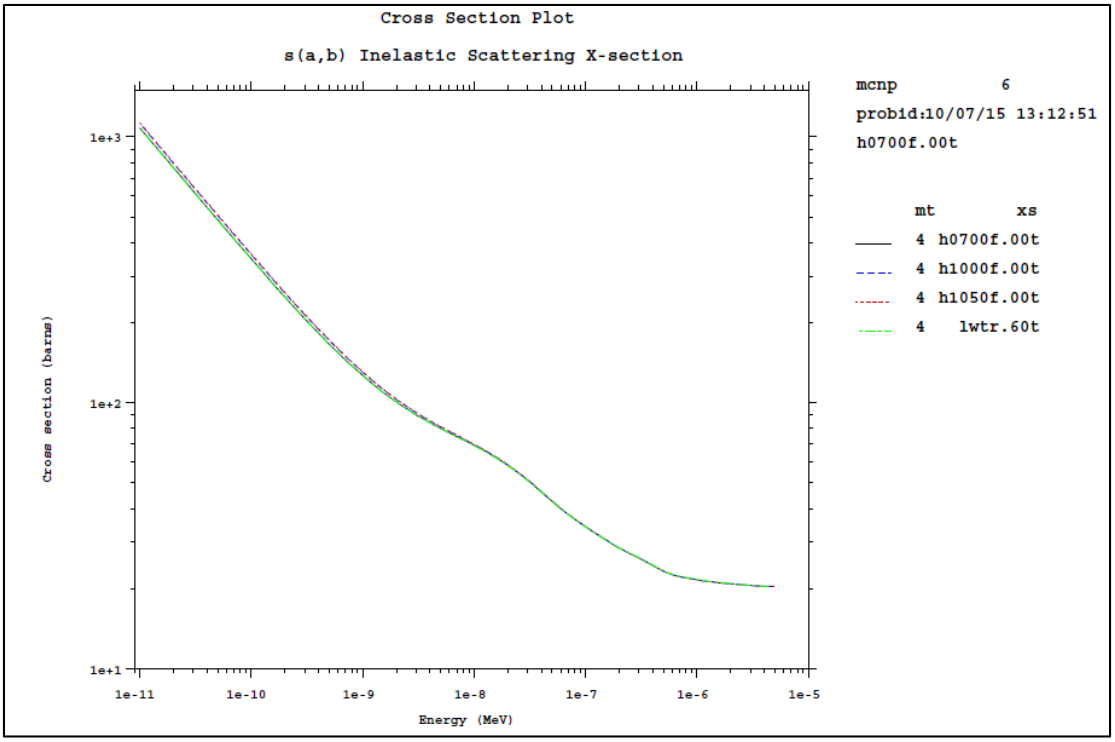

Figure 1. Comparison of the generated NJOY99 H in H_2O data with the default MCNP6 data library at 68.8°F [5].

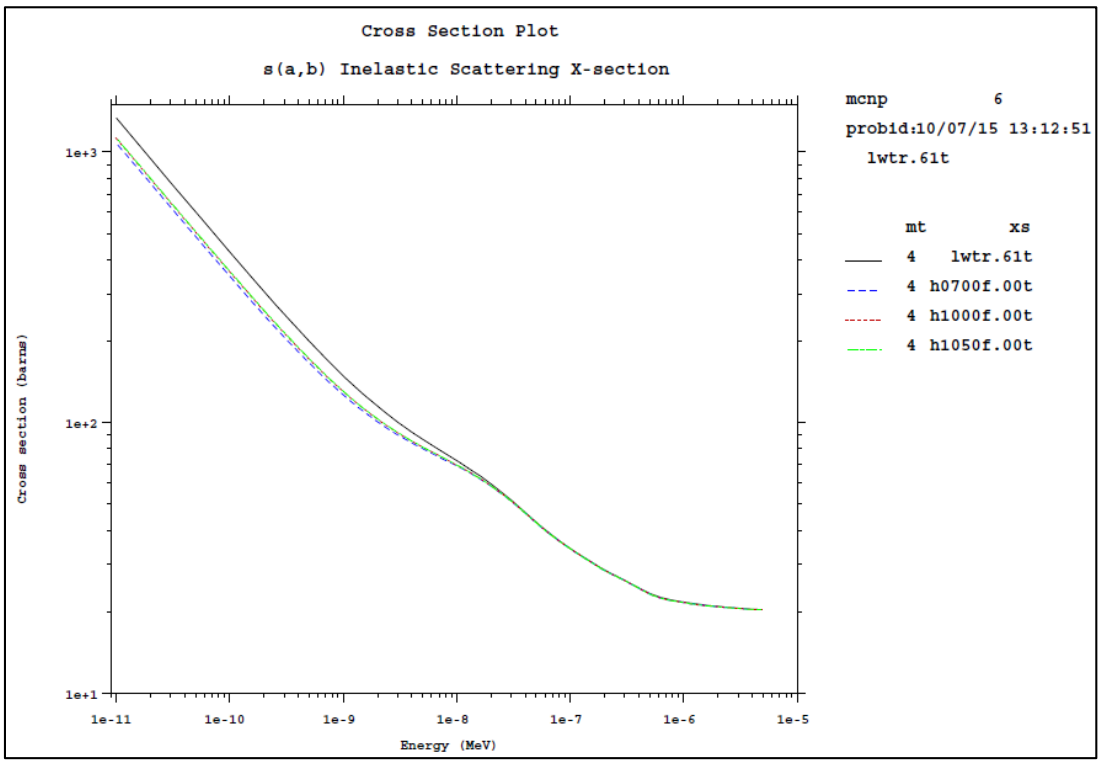

Figure 2. Comparison of the generated NJOY99 H in H_2O data with the default MCNP6 data library at 260 °F [5].

Total cross-section for ^{235}U are compared to the default MCNP6 library at 68.8 °F (92235.80c) in Figures 3 and 4. Table 8 lists the temperature corresponding to each library. Each exemplar energy region was selected to demonstrate the broadening effect. In the thermal region (1E-8 to 1E-6 MeV), temperature is not expected to have an effect; as may be observed in Figure 3. The resonance at 0.27 eV in this region has an approximate width of 46 meV, and is expected to be insensitive to Doppler broadening for temperatures below approximately 1000 ºF [6,7]. The resonance at 10.16 eV, in Figure 4, is nearly identical for the default MCNP6 library (92235.80c) and the library processed with NJOY99 at 70 ºF. Furthermore, the library processed with NJOY99 at 293 ºF demonstrates Doppler broadening of this ^{235}U resonance.

Table 8. ^{235}U Continuous Energy Cross-Section Libraries.

Library	Temperature (°F)
92235.80c	68.8
92235.11c (this work)	70
92235.07c (this work)	293

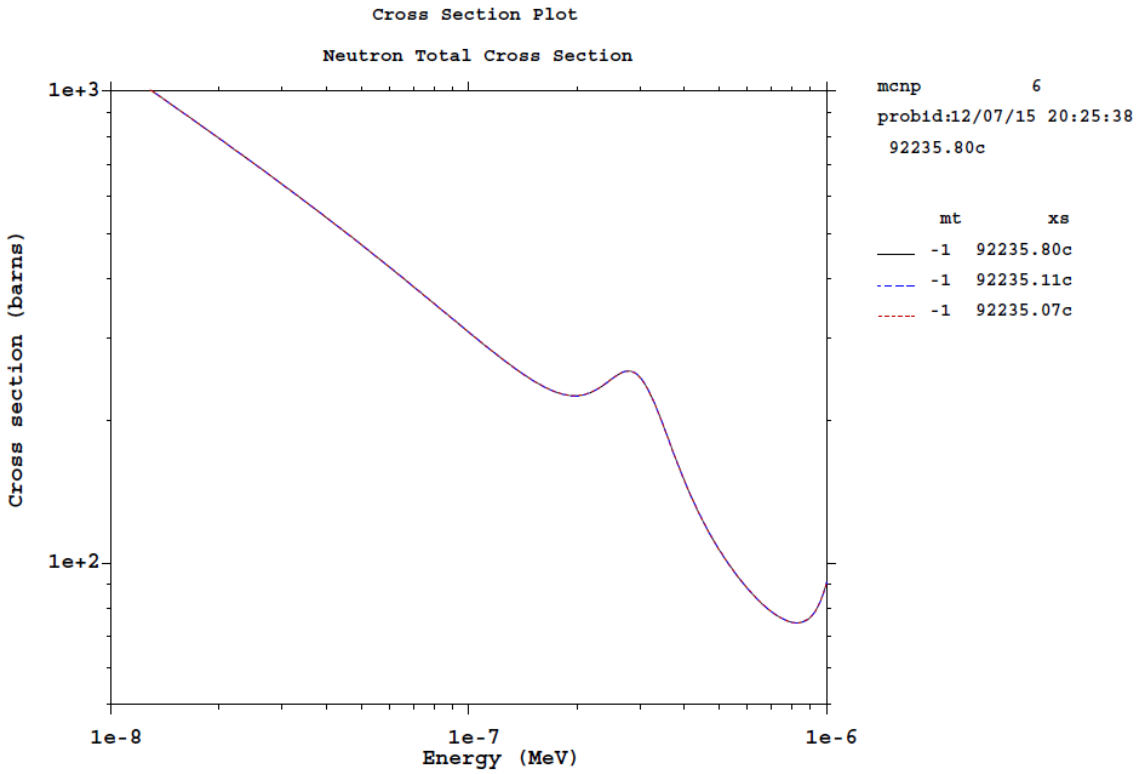

Figure 3. Comparison of the generated NJOY99 ^{235}U cross-section and the default MCNP6 library in thermal region.

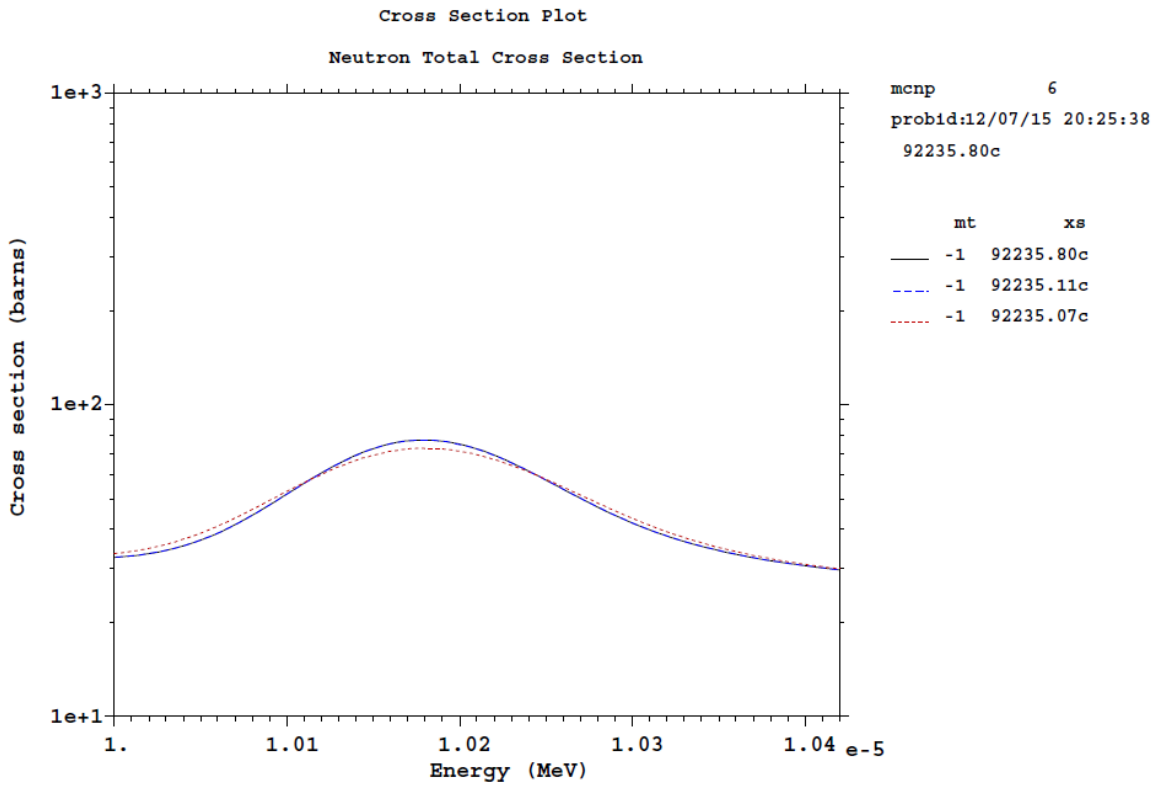

Figure 4. Comparison of the generated NJOY99 ^{235}U cross-section and the default MCNP6 library for 10.16 eV resonance.

Total cross-section for ^{238}U are compared to the default MCNP6 library at 68.8 °F (92238.80c) in Figures 5 and 6. Table 9 lists the temperature corresponding to each library. Each exemplar energy region was selected to demonstrate the broadening effect. In the thermal region (1E-8 to 1E-6 MeV), temperature was not observed to have an effect. The resonance at 6.67 eV, illustrated in Figure 5, is a representative resonance for Doppler broadening in ^{238}U. For this resonance, the default MCNP6 library (92235.80c) and the library processed with NJOY99 at 70 ºF (92238.11c) are nearly identical. Furthermore, the library processed with NJOY99 at 293 ºF (92238.07c) demonstrates Doppler broadening. A second exemplar resonance at 10.2 eV (Fig. 6), further demonstrates the expected effects in the NJOY99 processed libraries; where-by 92238.80c and 92238.11c are nearly identical, and 92238.07c is broadened.

Table 9. ^{238}U Continuous Energy Cross-Section Libraries.

Library	Temperature (°F)
92238.80c	68.8
92238.11c (this work)	70
92238.07c (this work)	293

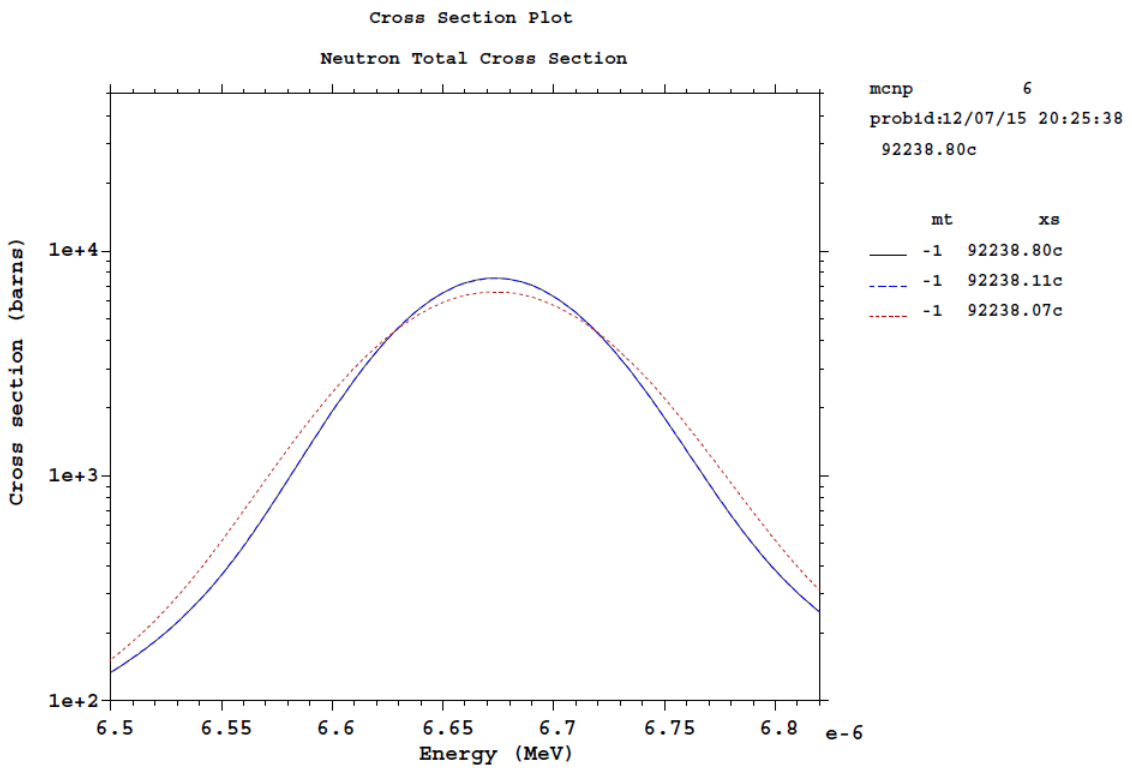

Figure 5. Comparison of the generated NJOY99 ^{235}U cross-section and the generic MCNP6 library for 6.67 eV resonance.

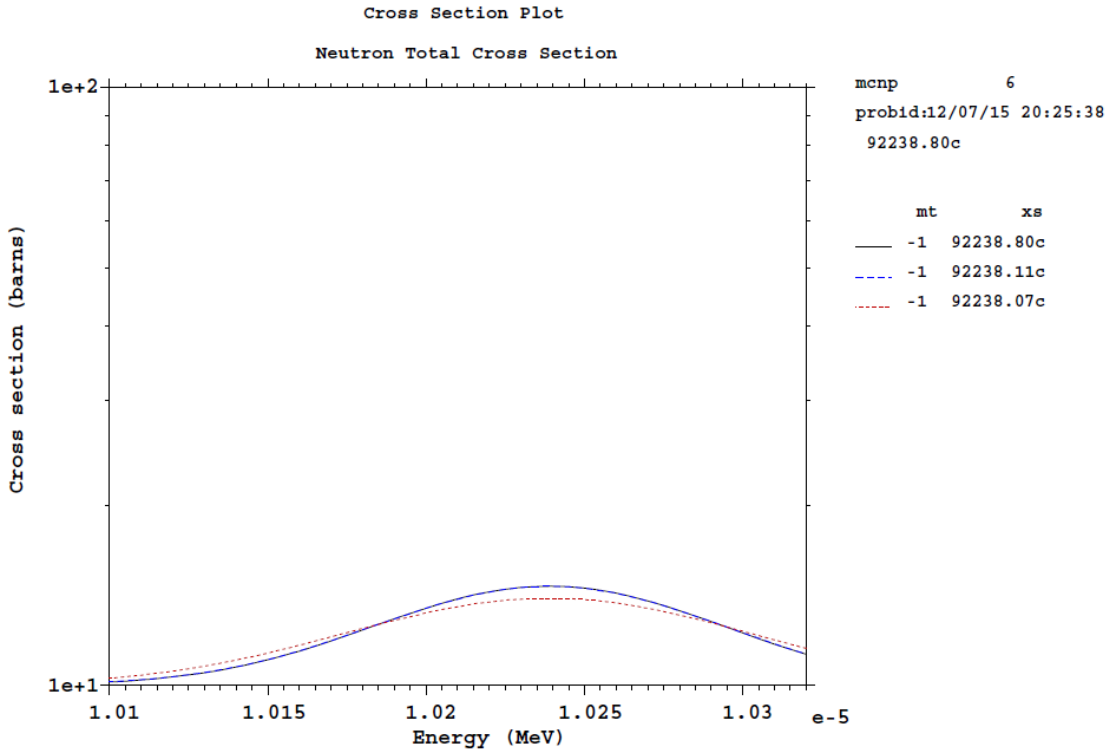

Figure 6. Comparison of the generated NJOY99 ^{235}U cross-section and the generic MCNP6 library for 10.2 eV resonance.

2) **Explain whether other benchmark cores were utilized, other than the initial fresh fuel core, to validate the core model and to calculate the uncertainty margin. If so, was the use of other benchmark cores documented in a separate report as part of the Verification and Validation of the MCNP6 code?**

In this work, the benchmark cores are all historical and current configurations of the PULSTAR core (i.e., the standard core through RC8). These 8 cores were modeled in detail (including depletion effects) and their behavior validated against a variety of measurements that were made on these specific cores (see Appendix A, Figure 3.2 and Table 3.2) showing reasonably good agreement. The resulting MCNP6 model was subsequently used to analyze the behavior of PULSTAR cores containing 4% and 6% enriched fuel.

h) **In the summary of parameter comparison of measured vs. calculated historic core configurations, the measured vs calculated parameters are relatively in good agreement, except for core configuration 8. Explain whether there are any unaccounted measurement or calculation errors that could be affecting the results for core configuration 8.**

Differences in the calculated and measured parameters for reflected core 8, tabulated in Table 3.2 of Appendix A, may be due to inaccuracies in the measurements of rod worth values. Flooding of beamport #6 during operation with reflected core 8 significantly affects both the available reactivity and rod worth values. While this beamport is empty, as is the case for most of the operation of RC8, the measured rod worth values are expected to be lower than when the beamport is flooded.

i) **Describe the predicted core reactivity parameters and power peaking behaviors for the core configuration using six weight percent fuel assemblies for the end of core burn-up calculations.**

Burn-up calculations were performed on RC9-2 for an operation time of 540 MWd, which is sufficient to decrease the excess reactivity from 3160 pcm to 1524 pcm (less than the required 1750 pcm for full power operation at 1 MW, see Appendix A, Table 1.3). These simulations were performed at 1 MW as defined in Appendx A, Table 1.1. As an example, the predicted core reactivity parameters for RC9-2 are shown in Table 10 below.

j) **Discuss the verifications of model geometry definition and input data as well as configuration changes for specific core analyses (i.e., fuel shuffling locations) that were performed.**

Geometry was verified through the use of the MCNP6 MCPLOT module to visualize the geometry and ensure the lack of errors. In addition, the use of common geometry for all models, and the establishment of cell and material identification conventions for new materials, minimized the opportunity for geometrical errors. In the creation of new models, geometry changes were visualized and verified for consistency within the input files.

Verification through the use of MCPLOT is demonstrated for the standard core and reflected core 8 in Figures 7 and 8, respectively. In each case, the cross-sectional 'slice' of the core is at the core mid-plane. Geometry cells are colored according to material. Consequently each unique fuel volume is distinguishable.

Table 10. Summary of MCNP6 predicted BOC and EOC core parameters for RC8 and RC9-2.

	Reflected Core 8 BOC	Reflected Core 8 EOC	Reflected Core 9-2 BOC	Reflected Core 9-2 EOC
α_T (pcm/^{o}F)	-3.39	-3.67	-3.44	-3.20
α_F (pcm/^{o}F)	-1.65	-1.65	-1.63	-1.66
α_V (pcm/cm^3)	-1.13	-1.03	-1.13	-1.18
α_P (pcm/MW)	-343	-329	-334	-340
β_{eff} (pcm)	731	751	733	721
F_Q	2.56	2.53	2.54	2.37

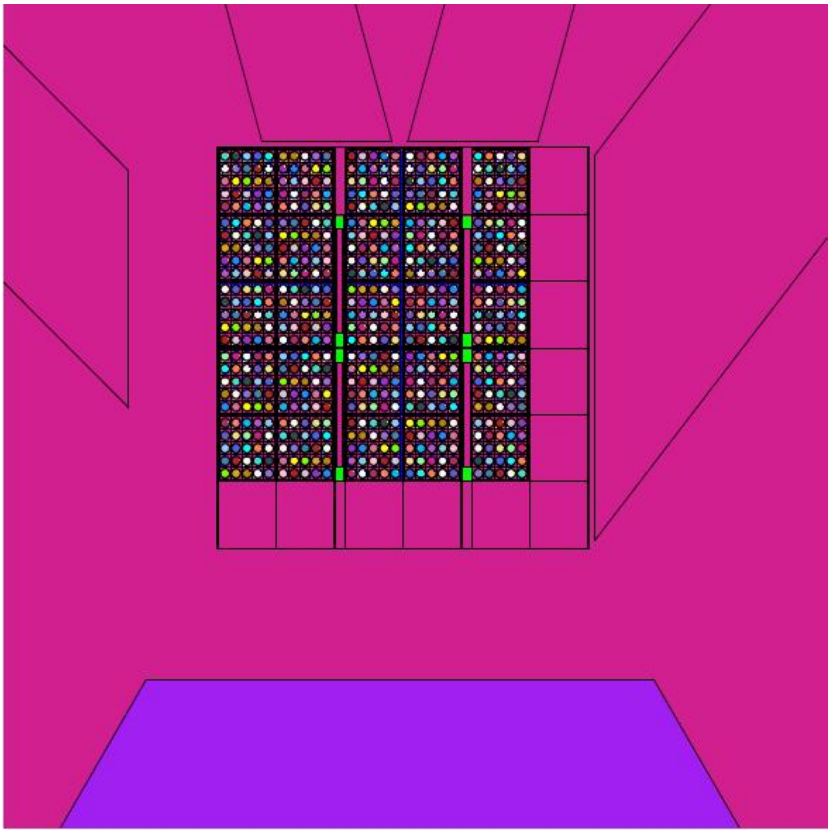

Figure 7. Cross-sectional geometry plot of the MCNP6 model of the PULSTAR in the standard core configuration. The cross-sectional 'slice' is through the core mid-plane.

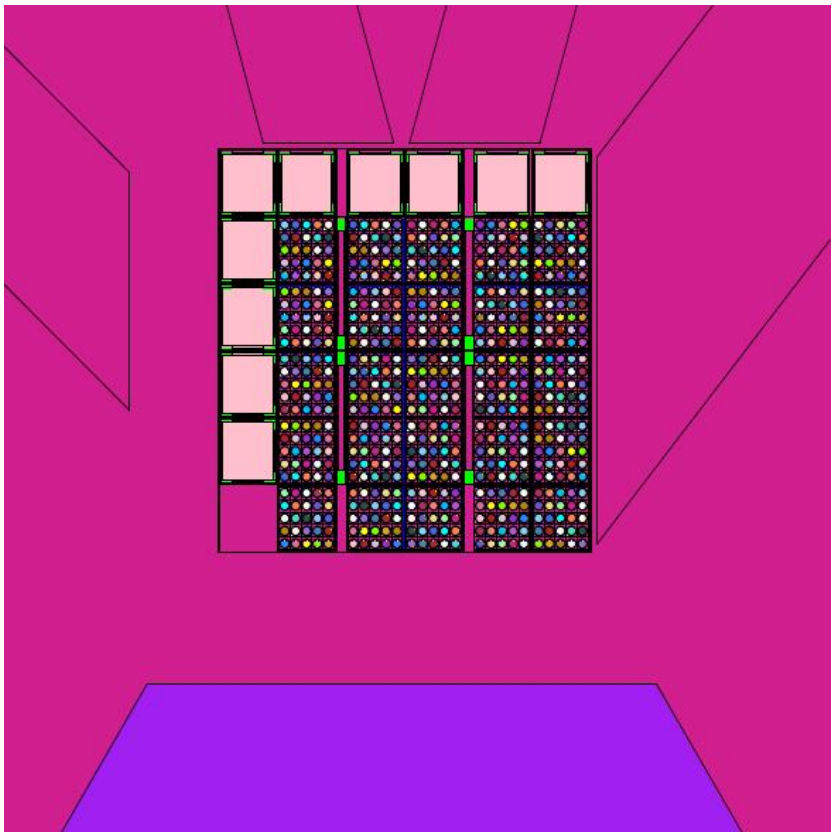

Figure 8. Cross-sectional geometry plot of the MCNP6 model of the PULSTAR in the reflected core 8 configuration. The cross-sectional 'slice' is through the core mid-plane.

k) Discuss the extent computer scripts were used to shuffle fuel assembly locations vs. manual data entry.

Computer scripts and codes were used extensively for fuel shuffling. The heavy use of universes in MCNP6 permitted the fuel to be moved with minimal changes to the input file. The material and cell identification convention were exploited in scripts to redefine material cards and fuel volume cell densities (to account for isotopes that were not tracked) between core configurations. Following the use of scripts to perform fuel shuffling, the data entries were verified by visual inspection. Shown below is a flow chart of the analysis process that was used for each core configuration.

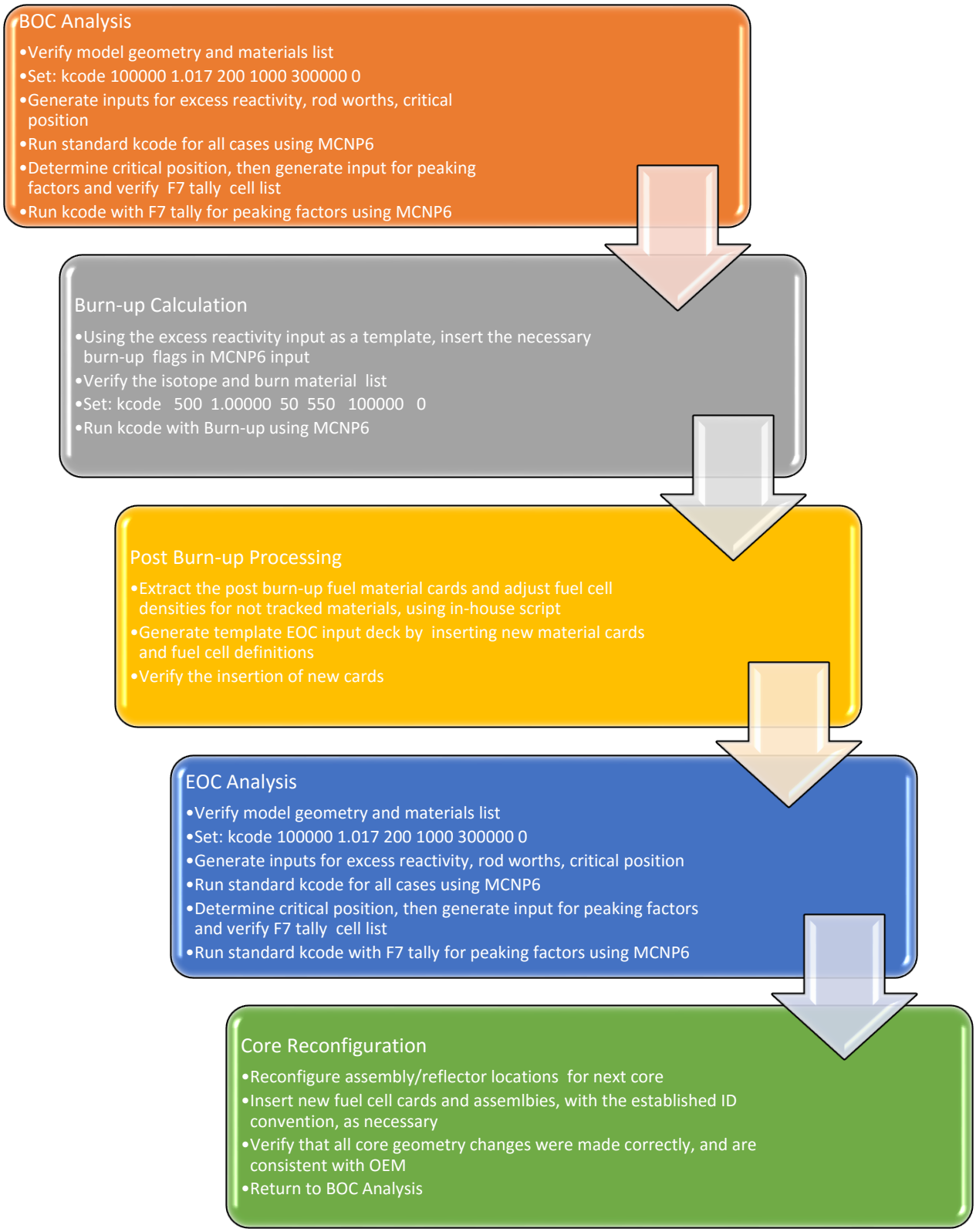
BOC Analysis
•Verify model geometry and materials list
•Set: kcode 100000 1.017 200 1000 300000 0
•Generate inputs for excess reactivity, rod worths, critical position
•Run standard kcode for all cases using MCNP6
•Determine critical position, then generate input for peaking factors and verify F7 tally cell list
•Run kcode with F7 tally for peaking factors using MCNP6
Burn-up Calculation
•Using the excess reactivity input as a template, insert the necessary burn-up flags in MCNP6 input
•Verify the isotope and burn material list
•Set: kcode 500 1.00000 50 550 100000 0
•Run kcode with Burn-up using MCNP6
Post Burn-up Processing
•Extract the post burn-up fuel material cards and adjust fuel cell densities for not tracked materials, using in-house script
•Generate template EOC input deck by inserting new material cards and fuel cell definitions
•Verify the insertion of new cards
EOC Analysis
•Verify model geometry and materials list
•Set: kcode 100000 1.017 200 1000 300000 0
•Generate inputs for excess reactivity, rod worths, critical position
•Run standard kcode for all cases using MCNP6
•Determine critical position, then generate input for peaking factors and verify F7 tally cell list
•Run standard kcode with F7 tally for peaking factors using MCNP6
Core Reconfiguration
•Reconfigure assembly/reflector locations for next core
•Insert new fuel cell cards and assemlbies, with the established ID convention, as necessary
•Verify that all core geometry changes were made correctly, and are consistent with OEM
•Return to BOC Analysis

References

[1] Specifications for PULSTAR Fuel Assemblies, American Machine & Foundry Co., York Division, April 1970 (York, Pennsylvania).

[2] Safety Analysis Report, North Carolina State University PULSTAR Reactor, License No. R-120, Docket No. 50-297 (1997).

[3] Buffalo Materials Research Center Hazards Summary Report, Revision II, September 23, 1963.

[4] Buffalo Materials Research Center Safety Evaluation Report, NUREG-0982, May 1983.

[5] LA-UR-13-21822v1_ace_list

[6] M. B. Chadwick et al., *Nuclear Data Sheets*, vol. 112, 2887 (2011).

[7] R. E. MacFarlane, D. W. Muir, "The NJOY Nuclear Data Processing System Version 91," Los Alamos National Laboratory report LA-12740-M (1994).